Journal of Rehabilitation in Civil Engineering 6-1 (2018) 01-09

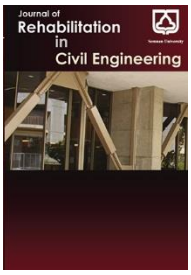

Journal homepage: http://civiljournal.semnan.ac.ir/

Numerical Investigation of Geometric Parameters Effect of the Labyrinth Weir on the Discharge Coefficient

S. Emami[1*], H. Arvanaghi[1] and J. Parsa[1]
1.Water Engineering Department, Faculty of Agriculture, University of Tabriz, Tabriz, Iran

Corresponding author:somayehemami70@gmail.com

ARTICLE INFO

Article history:
Received: 23 May 2017
Accepted: 09 July 2017

Keywords:
Labyrinth Weir,
Discharge Coefficient,
Computational Fluid Dynamics,
Fluent.

ABSTRACT

Weirs, as overflow structures, are extensively applied for the measurement of flow, its diversion, and control in the open canals. Labyrinth weir as a result of more effective length than conventional weirs allows passing more discharge in narrow canals. Determination of the design criteria for the practical application of these weirs needs more examination. Weir angle and its position relative to the flow direction are the most effective parameters on the discharge coefficient. In this article, Fluent software was applied as a virtual laboratory, and extensive experiments were carried out to survey the effect of geometry on the labyrinth weir discharge coefficient. The variables were the height of weir, the angle of the weir, and the discharge. The discharge coefficients acquired from these experiments were then compared with the corresponding values obtained from the usual rectangular sharp-crested weir experiments. Comparison of the results indicated that in all cases with different vertex angle, flow discharge coefficients are in a satisfactory range for relative effective head less than 0.3. The discharge coefficient is reduced for relative effective head more than 0.3 due to the collision of water napes. It revealed that the higher the weir, the more discharge capacity. As a result, the labyrinth weirs have a better performance in comparison with the common sharp-crested.

1. Introduction

The labyrinth weir is one of the most economical weirs, because of its optimal discharge capacity in comparison with construction costs in other weirs. The great advantages of linear crest weirs are their simplicity in construction and maintenance:

$$Q = \frac{2}{3} C_d \sqrt{2g}\, L H^{1.5} \quad (1)$$

Where L = crest length of the weir, C_d= discharge coefficient, g = acceleration as a

DOI: 10.22075/JRCE.2017.11428.1188

result of the gravity and H= static head over the crest.
The C_d depends on the flow characteristics and geometry of the canal and weir (Kumar et al., 2013).

Several laboratory studies have been conducted on labyrinth weirs. Hay and Taylor (1970) examined various performances of labyrinth weirs. They examined the effect of bottom slope on the overflow capacity of labyrinth weirs, and the influence of water head over the weir crest [2]. Darvas (1971) proposed a definition for the discharge coefficient of labyrinth spillways. Houston and Hinchliff (1982) investigated the several labyrinth spillways for Hyrum dam by means of physical modeling of 45 different states. The study of Cassidy et al. (1985) on the performance of labyrinth spillways for high water head showed a 20% reduction in efficiency of the spillways. Naseri (2003) compared the discharge coefficient of labyrinth weirs for different crest shapes and lengths applied to physical modeling. He indicated that the semi-circle crest shape has the highest discharge coefficient [3]. Carollo et al. (2012) also investigated the discharge capacity of triangular labyrinth weirs with different geometrical characteristics in a laboratory flume [3].
Emiroglu and Kisi (2013) predicted discharge coefficient of trapezoidal labyrinth side weirs applying ANFIS. Results exhibited ANFIS model is more optimal.
Seamons (2014) examined the effects of geometric design parameters of varying certain labyrinth weir to compute their effects on discharge efficiency. The purpose of this study was to determine the effects of varying certain labyrinth weir geometric design parameters to specify the effects on discharge efficiency.
Roushangar et al. (2017) investigated the discharge coefficient of normal and inverted orientation labyrinth weirs using machine learning techniques. The results indicated that Fr in the GEP model and Fr and H_T/Pin the ANFIS model is the most effective variables for determining Cd for normal and inverted orientation labyrinth weirs, respectively.
Roushangar et al. (2017) applied support vector machine method to compute the discharge coefficient of the labyrinth and arced labyrinth weirs. Results of this study indicate the vector machine method is the most effective method for acquired discharge coefficient of the labyrinth.
In recent years, progresses in computational fluid dynamics (CFD) algorithms and developments in computer hardware caused evolving new tools for evaluation of different flow conditions and different design alternatives. Savage et al. (2004) and Danish hydraulic institute (DHI) (2005) examined the flow past the labyrinth spillways applying numerical simulation. Crookston (2012) performed numerical simulation on the multi-dimensional labyrinth weirs. They used previous physical model results on a rectangular flume under laboratory conditions. They performed, then, a three-dimensional simulation of flow over the weir applied Flow-3D Software. The objective of their study was indicating the capability of Reynolds Averaged Navier-Stokes equations in the modeling of flow turbulence over the Labyrinth weirs. Due to the importance of accurate modeling of the free-surface, a two-phase flow, i.e., water and air, was utilized. Thus, the robust volume of fluid (VOF) technique was used to determine the location and orientation of the interface between the water and air, i.e., free surface.
In this paper, we examined the effects of the geometric parameters on the discharge coefficient of labyrinth weirs. This study is aimed to specify a range for the geometric parameters in which the weir discharge coefficient remains constant.

2. Materials and Methods

2.1. Labyrinth Weir

Labyrinth weirs are very easy to design and have more effective length than the common sharp-crested weirs. They would be able to

pass more discharge in comparison with the usual weirs for the same length and head of water. Figure (1) depicted a sketch of Labyrinth weir, related parameters, and the section view of flow over the weir.

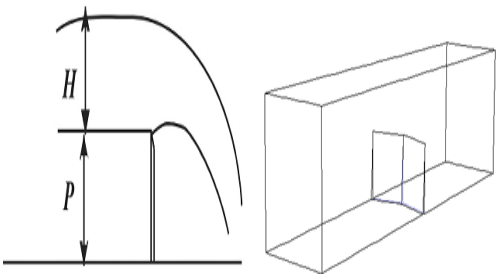

Fig. 1. Labyrinth weir and the corresponding parameters; (a) plan view; (b) section view of flow over Labyrinth weir.

2.2. Governing Equations

The governing equations of flow over weirs are the well-known Navier- Stokes equations; a continuity equation and three momentum equations in the three-dimensional state. By including the effect of turbulence, the equations change to Reynolds equations as [Wilcox and David, 2006]:

Continuity equation:

$$\frac{\partial U_i}{\partial x_i} = 0 \tag{2}$$

Momentum equation:

$$\rho \frac{\partial U_i}{\partial x_i} + \rho \frac{\partial}{\partial x_j}\left(U_j U_i + \overline{u'_j u'_i}\right) \tag{3}$$

in which U_i is average velocity in (i) direction, P is pressure, μ is Molecular viscosity, ρ is the density of water, S_{ji} is Strain-rate tensor, $\overline{u'_j u'_i}$ is time-averaged momentum due to turbulence, which is called Reynolds stresses. $\rho\overline{u'_i u'_j}$ has nine components [Wilcox and David,2006]:

$$\rho\overline{u'_i u'_j} = \begin{bmatrix} \rho\overline{(u'_1{}^2)} & \rho\overline{u'_1 u'_2} & \rho\overline{u'_1 u'_3} \\ \rho\overline{u'_2 u'_1} & \rho\overline{(u'_2{}^2)} & \rho\overline{u'_2 u'_3} \\ \rho\overline{u'_3 u'_1} & \rho\overline{u'_2 u'_3} & \rho\overline{(u'_3{}^2)} \end{bmatrix} \tag{4}$$

These unknowns, as a result of the turbulence, are determined by using turbulence models. These models consist of semi-empirical equations which relate the fluctuating components of quantities to the average components. The most popular turbulence model is the k-ε model. The RNG scheme of this model can be applied to solve Reynolds stresses.

There are different methods to solve RANS equations. In this study, the k-ε RNG turbulence model is used, which is defined as (Papageorgakis and Assanis, 1999):

$$\frac{\partial}{\partial t}(\rho k) + \frac{\partial}{\partial x_i}(\rho k u_i) = \frac{\partial}{\partial x_j}\left(\alpha_k \mu_{eff} \frac{\partial k}{\partial x_j}\right) + G_k + G_b - \rho\varepsilon - Y_M + S_k \tag{5}$$

$$\frac{\partial}{\partial t}(\rho\varepsilon) + \frac{\partial}{\partial x_i}(\rho\varepsilon u_i) = \frac{\partial}{\partial x_j}\left(\alpha_k \mu_{eff} \frac{\partial \varepsilon}{\partial x_j}\right) + C_{1\varepsilon}\frac{\varepsilon}{k}(G_k + C_{3\varepsilon} G_b) - C_{2\varepsilon}\rho\frac{\varepsilon^2}{k} - R_\varepsilon + S_\varepsilon \tag{6}$$

where k is kinetic energy, ε is energy dissipation rate, G_k is turbulence kinetic energy generation due to mean velocity gradient, G_b is kinetic energy due to floatation, Y_M is turbulence Mach number and the other parameters are model coefficients and:

$$R_\varepsilon = \frac{C_\mu \rho \eta^3 \left(1-\frac{\eta}{\eta_0}\right)}{1+\beta\eta^3}\frac{\varepsilon^2}{k} \tag{7}$$

$$C_\eta = \frac{\eta\left(1-\frac{\eta}{\eta_0}\right)}{1+\beta\eta^3} \tag{8}$$

These unknowns are computed by using the turbulence modeling process.

2.3. Volume of Fluid (VOF) Approach

This approach was first introduced by Hirt and Nichols in 1981 (Hirt et al., 1981). In this approach, the fraction of computational cells occupied by each fluid, e.g., water and air, and the position of the interface between fluids were determined. The location of the interface is calculated by applying the following equations (Chen et al., 2002):

$$\frac{\partial \alpha_w}{\partial t} + u_i \frac{\partial \alpha_w}{\partial x_i} = 0 \tag{9}$$

$$\alpha_a = 1 - \alpha w \tag{10}$$

Which α_w and α_a are respectively the fractions of water and air within a cell. The above equations are for a two-phase flow which

consists of water and air; the subscript "w" refers to water and "a" refers to air. The momentum equation for this two-phase flow is similar to that of for a single flow which expressed by Navier- Stokes equations. But ρ (density) and μ (molecular viscosity) should be modified due to the variations of each fluid fraction. Consequently, they may be written as (Anoymous, 2006):

$$\rho = \alpha_w \rho_w + (1 - \alpha_w)\rho_a \quad (11)$$

$$\mu = \frac{\alpha_w}{\mu_w} + (1 - \alpha_w)\mu_a \quad (12)$$

in which ρ_a and ρ_w are the density of air and water, while μ_a and μ_w are the molecular viscosity of air and water, respectively (Anoymous, 2006).

2.4. Numerical Solution

In this study, numerical modeling is carried out by Fluent v. 6.2. Fluent in one of the powerful and common CFD commercial software. It first transforms the governing equations to the algebraic equations by finite volume method then solves them. Fluent has the ability to solve 2D and 3D problems of open canal flow, confined conduit flow, and sediment transport by the turbulence models. Moreover, it is possible to explain continuum and momentum equations so-called Navier- Stocks equations around Labyrinth weirs. The experiments were conducted in a canal of length 4.5 m, width 0.5 m, and depth 0.6 m. To solve the partial differential governing equations, fluent employs the Finite Volume Method. Discretization of the governing equations can be done by applying the upwind method. The simulated velocity and pressure fields are coupled by using the "Piso" method. To start Fluent modeling, we first need to determine the canal geometry and then generate a mesh for it. Gambit software is applied to generate the mesh. GAMBIT Software is used for geometrical construction and grid generation of the numerical model through which user can depict and generate grids for the contemplated model with the highest accuracy. This software has a set of commands for the rapid organization of 2D and 3D geometries. It also includes structural and unstructured meshes. In general, the generation of grids in GAMBIT is carried out as:

1. Creating the geometry of the problem
2. Generating the grid of created geometry
3. Defining the related boundary conditions
4. Meshing the geometrical model of labyrinth weir using Gambit is depicted in Figure (2).

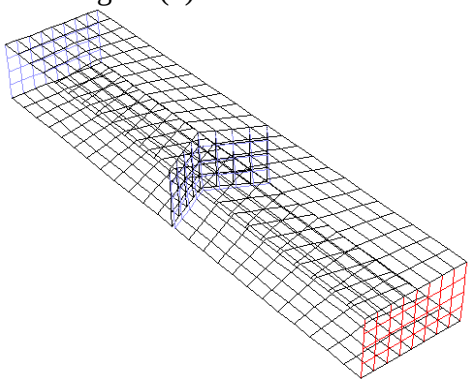

Fig. 2. Meshing the geometrical model of Labyrinth weir applying GAMBIT.

Suitable boundary conditions are of primary importance. These are illustrated in Figure (3).

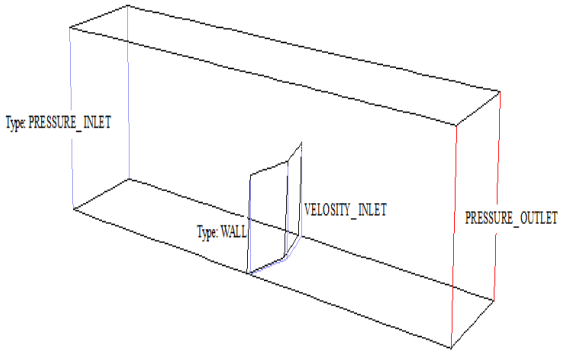

Fig. 3. Boundary conditions used in simulation throughout the domain.

A water inlet: pressure inlet boundary condition was used to define the water pressure at flow inlets. This boundary condition is based on the assumption that upstream inlet is sufficiently far away from the crest where velocity is negligible. For the leading walls at two sides of flow as well as for the bottom, the

wall boundary condition is assigned to bound fluid and solid regions. For downstream, a pressure outlet boundary was contemplated to determine static pressure at the outlet.
Discharge equation for a labyrinth weir can be obtained as follows:

$$Q = \frac{2}{3} Cd\, L \sqrt{2g} H_0^{3/2} \quad (13)$$

In which, L and H_o are the effective length of the weir and total head on the crest, respectively. L is defined in consonance with the geometry of the weir, and total head (H_o) is defined as the summation of the static head ($P/\rho g$) and velocity head ($U^2/2g$) that are computed once the pressure and velocity fields are computed by the numerical solution. Subsequently, the discharge coefficient, C_d, can be acquired (Zahraeifard V and Talebeydokhti, 2012).

2.5. Dimensional Analysis

The flow discharge of the weir is a function of several parameters (Figure 1), which is mathematically expressed by the equation as follows:

$$C_d = f(H_d, L_e, P, W, \theta, y) \quad (14)$$

WhereH_d is the total head over the weir crest, W is the weir width, P is the height of the weir, θ is the vertex angle, and y is the flow depth. Dimensional analysis is performed to find a relation between the discharge coefficient and other parameters stated above. Below a mathematical expression of this relation is given:

$$C_d = f\left(F_r, \frac{H_d}{P}, \frac{L_e}{P}, \frac{y}{P}, \frac{H_d}{w}, \frac{y}{w}, R_e, \frac{L_e}{w}, \theta, W_e\right) \quad (15)$$

3. Results and Discussions

The numerical simulations were performed for the weirs of vertex angle θ = 30◦, 60°, 90°, 120°, 150°, and 180° and two different heights of Labyrinth weirs of the same width of the canal. The ranges of the data are given in Table 1.

Variation of C_d with H/P is portrayed in Fig. 4 for the weirs of different vertex angles. It can be noted that C_d decreases by decreasing the vertex angle due to the collision of the falling jets for the high value of H/P. However, for the low value of H/P, the collision of jets is not so severe, resulting in high values for C_d. As a result, by increasing the vertex angle, the reduction rate of C_d with H/P decreases.

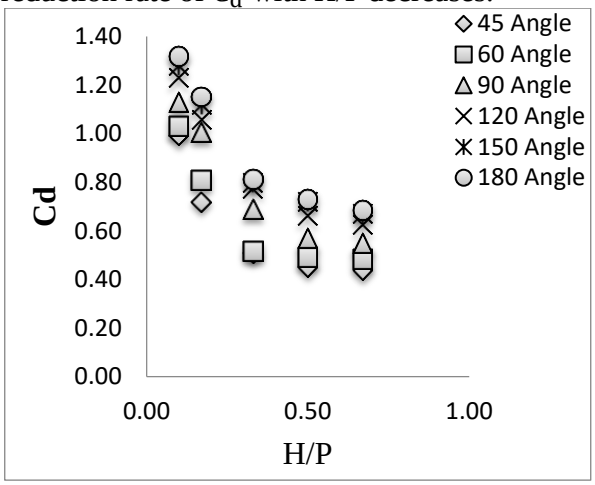

Fig. 4. The Numerical results of the C_d at various θ.

Variation of discharge with head over the crest for the Labyrinth weirs of different vertex angles is illustrated in Fig. 5. This figure indicates that for the same value of h, discharge increases with the reduction of vertex angle due to the growth of the crest length of the weir.

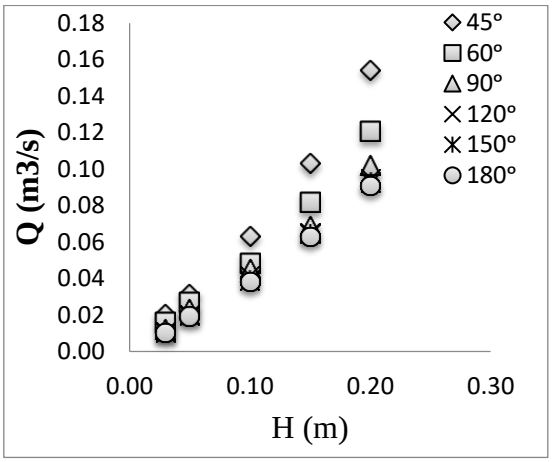

Fig. 5. Variation of Q with H for Labyrinth weir of the different vertex angle.

Table1. Results of the simulations in the present study.

No.	Θ (°)	L (m)	H (m)	P (m)	H/P	C_d	Q (L/S)
W1	45	1.32	0.03	0.3	0.1	0.992	20.1926
W2	45	1.32	0.05	0.3	0.17	0.720	31.5345
W3	45	1.32	0.1	0.3	0.33	0.509	63.0545
W4	45	1.32	0.15	0.3	0.5	0.530	103.094
W5	45	1.32	0.2	0.3	0.67	0.730	154.1686
W6	60	1	0.03	0.3	0.1	1.030	15.8834
W7	60	1	0.05	0.3	0.17	0.809	26.8428
W8	60	1	0.1	0.3	0.33	0.517	48.5193
W9	60	1	0.15	0.3	0.5	0.473	81.5497
W10	60	1	0.2	0.3	0.67	0.460	120.776
W11	90	0.7	0.03	0.3	0.1	1.130	12.1978
W12	90	0.7	0.05	0.3	0.17	1.007	23.3887
W13	90	0.7	0.1	0.3	0.33	0.690	45.3285
W14	90	0.7	0.15	0.3	0.5	0.570	68.7914
W15	90	0.7	0.2	0.3	0.67	0.550	102.1951
W16	120	0.57	0.03	0.3	0.1	1.230	10.8115
W17	120	0.57	0.05	0.3	0.17	1.060	20.0475
W18	120	0.57	0.1	0.3	0.33	0.775	41.4573
W19	120	0.57	0.15	0.3	0.5	0.662	65.0570
W20	120	0.57	0.2	0.3	0.67	0.625	94.4636
W21	150	0.52	0.03	0.3	0.1	1.280	10.2641
W22	150	0.52	0.05	0.3	0.17	1.120	19.3242
W23	150	0.52	0.1	0.3	0.33	0.800	39.041
W24	150	0.52	0.15	0.3	0.5	0.721	64.6398
W25	150	0.52	0.2	0.3	0.67	0.671	92.6180
W26	180	0.5	0.03	0.3	0.1	1.132	10.1778
W27	180	0.5	0.05	0.3	0.17	1.153	19.1284
W28	180	0.5	0.1	0.3	0.33	0.812	38.1022
W29	180	0.5	0.15	0.3	0.5	0.730	62.9295
W30	180	0.5	0.2	0.3	0.67	0.684	90.7811

3.1. The Effect of the Height of Weir on the Discharge Coefficient

Figure 5 and 6 represents the dimensionless height of weir effect on the discharge coefficient. As presented in figure 6 and 7, by raising the height of weir, the discharge coefficient increase and the value of the discharge coefficient is constant after H/P =0.3 and is fixed by 0.47.

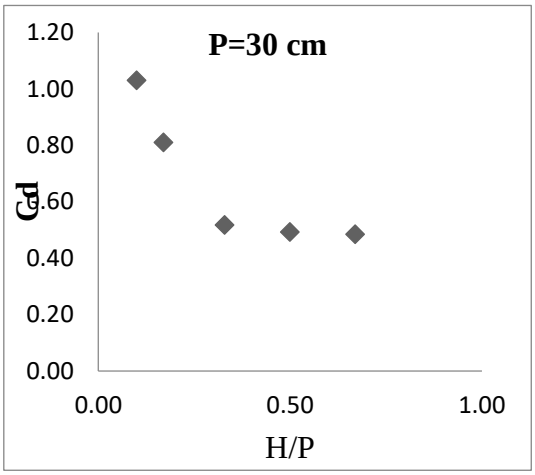

Fig. 6. The Numerical results of the C_d at various H/P (P=30 cm).

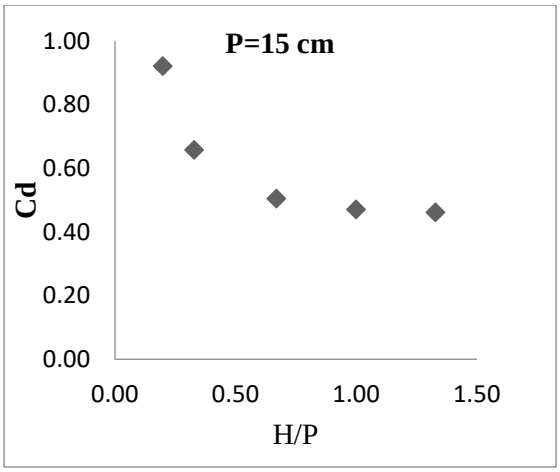

Fig. 7. The Numerical results of the C_d at various H/P (P=15 cm).

3.2. The Efficiency of the Labyrinth Weir

A hydraulic criterion for selecting a proper weir is its flow capacity in the same conditions, e.g., water head and weir length. To examine the efficiency of Labyrinth weir for different vertex angles, the ratio of discharges over the Labyrinth weir to the discharges over the usual rectangular sharp-crested weir, i.e., increase flow percent (Q%), is represented with H/Pin Fig. 8. The efficiency of Labyrinth weir is high for low vertex angle. It decreases with the growth of H/P as a result of the collision of the falling jets. For H/P= 0.3, the efficiency of Labyrinth weir is low, and even for $\theta = 45^{\circ}$, the efficiency is only 1.5 times to the usual rectangular sharp-crested weir.

3.3. Discharge Equation for Labyrinth Weir

Based on the obtained fitting of the resulted data by the numerical model, the discharge coefficient equation for Labyrinth weir can be acquired as follows:

$$C_d = 0.0948 \left(\frac{H}{P}\right)^{-0.249} \theta^{0.374} \quad (16)$$

As observed in the equation, the determination coefficient of the equation equals 96% (which is acceptable) applying linear fitness.

Above equation, with error value of 0.01695; was presented as the best equation to estimate the discharge coefficient over duckbill weirs. The application range of this equation is $45^{\circ} \leq \theta \leq 180^{\circ}$and $0.1 \leq \frac{H}{P} \leq 0.67$.

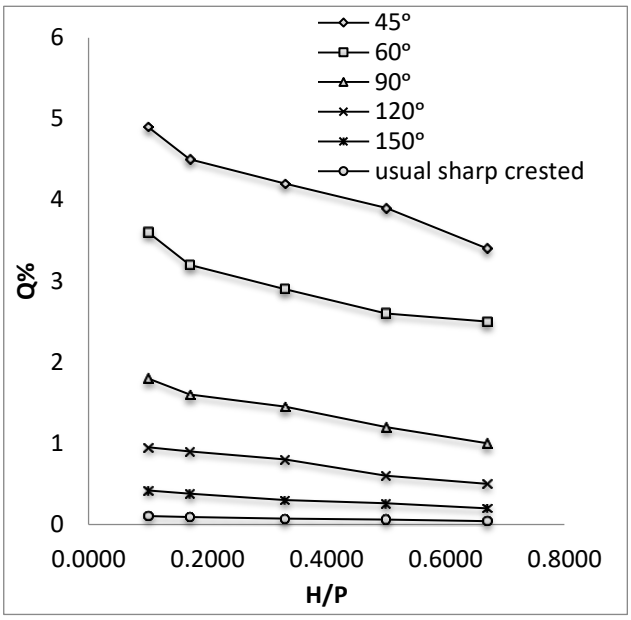

Fig. 8. Comparison variation of Q% with H/P for the Labyrinth weir of different vertex angle and usual sharp-crested weir.

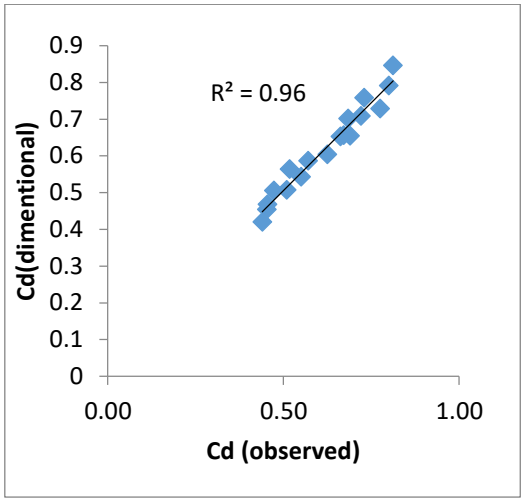

Fig. 9. The predicted values of the C_d at various observed values of C_d.

4. Conclusions

Labyrinth weir is a kind of non-linear weirs which are applied to control and measure the flow in open channels where the width of the

channel is low. In this study, we examined the effects of Labyrinth weir geometric parameters on the discharge coefficient. To this end, Fluent software was used, as a virtual laboratory, in order to simulate the different conditions of alabyrinth weir. The variables were the height of weir, the angle of the weir, and the discharge. The results indicated that the discharge coefficient decreases with the vertex angle. However, for low values of H/pand vertex angle, the C_d is high. By increasing the height of weir, the discharge coefficient increase, and the value of discharge coefficient remains0.47 for H/P >0.3. The regression analysis displayed that the vertex angle of the weir is the essential design parameter for labyrinth weirs. The efficiency of the Labyrinth weir is high for low vertex angle, and it decreases with the growth of H/Pdue to the collision of the falling jets.

REFERENCES

[1] Hirt, C. W. and Nichols, B. D. (1981). "Volume of Fluid (VOF) Method for the Dynamics of Free 274 Boundaries", Journal of Comput. Phys, Vol. 39(1), pp. 201-225.

[2] Kumar, S., Ahmad,Z., Mansoor,T and Himanshu,S. K.(2013). "A New Approach to analyze the flow over sharp crested curved plan form weir." International Journal of Recent Technology and Enginnering (IJRTE), Vol. 2,pp. 2277-3878.

[3] Hay, N., Taylor, G. (1970). "Performance and design of labyrinth weirs." ASCE, Journal of Hydraulics Division, Vol. 96(11), pp. 2337–57.

[4] Crookston B. M., Paxson, G. S. and Savage, B. M. (2012). "Hydraulic performance of labyrinth weirs for high headwater ratios.4th IAHR". International Symposium on Hydraulic Structures, Porto, Portugal, pp. 1–8.

[5] Shaghaghian R. S., Sharif, M. T. (2015). "Numerical modeling of sharp-crested triangular plan form weirs using FLUENT." Indian Journal of Science and Technology, Vol. 8(34), DOI: 10.17485/ijst/2015/v8i34/78200.

[6] Emiroglu, M. E., Kisi, O. (2013). "Prediction of discharge coefficient for trapezoidal labyrinth side weir using a neuro-fuzzy approach." Water Resources Management, Vol. 27(5), pp. 1473-1488.

[7] Seamons, T. R. (2014). "LabyrinthWeir: A look into geometric variation and its effect on efficiency and design method predictions." M. S. thesis, Utah State University, Logan, UT.

[8] Roushangar, K., Alami, M. T., MajediAsl, M. and Shiri, J. (2017). "Modeling discharge coefficient of normal and inverted orientation labyrinth weirs using machine learning techniques." ISH Journal of hydraulic engineering. Homepages://www.tandfonline.com/loi/tish20.

[9] Roushangar, K., Alami, M.T., Shiri, J. and MajediAsl, M. (2017). "Determining discharge coefficient of labyrinth and arced labyrinth weirs using support vector machine." Journal of Hydrology Research, Available Online: 2017 Mar, nh2017214; DOI: 10.2166/nh. 2017.214.

[10] Papageorgakis G. C., Assanis, D. N. (1999). "Comparison of linear and nonlinear RNG-based models for incompressible turbulent flows." Journal of Numerical Heat Transfer, University of Michigan, Vol. 35, pp. 1-22.

[11] Wilcox., David, C. (2006)."Turbulence Modeling for CFD." DCW Industries, Inc., La Canada, CA, 270 USA.

[12] Zahraeifard, V. and Talebeydokhti, N. (2012). "Numerical Simulation of Turbulent Flow over Labyrinth Spillways/Weirs." International Journal of Science and Tecnology, Vol. 22(5), pp.1734-1741.

[13] Anoymous. (2006). "Fluent 6.3 User's Guide. Chap. 23. Fluent Incorporated." Lebanon.

[14] Danish Hydraulic Institute website (DHI)<http://ballastwater.dhigroup.com/ 268 /media/publications/news/2009/07059ns3.pdf>. (Visited Aug. 17, 2010).

[15] Savage, B. M., Frizell, K. and Crowder, J. (2004). "Brains versus Brawn: The Changing World of 265 Hydraulic Model Studies". Proc. of the ASDSO Annual Conference, Phoenix, AZ, USA 266.